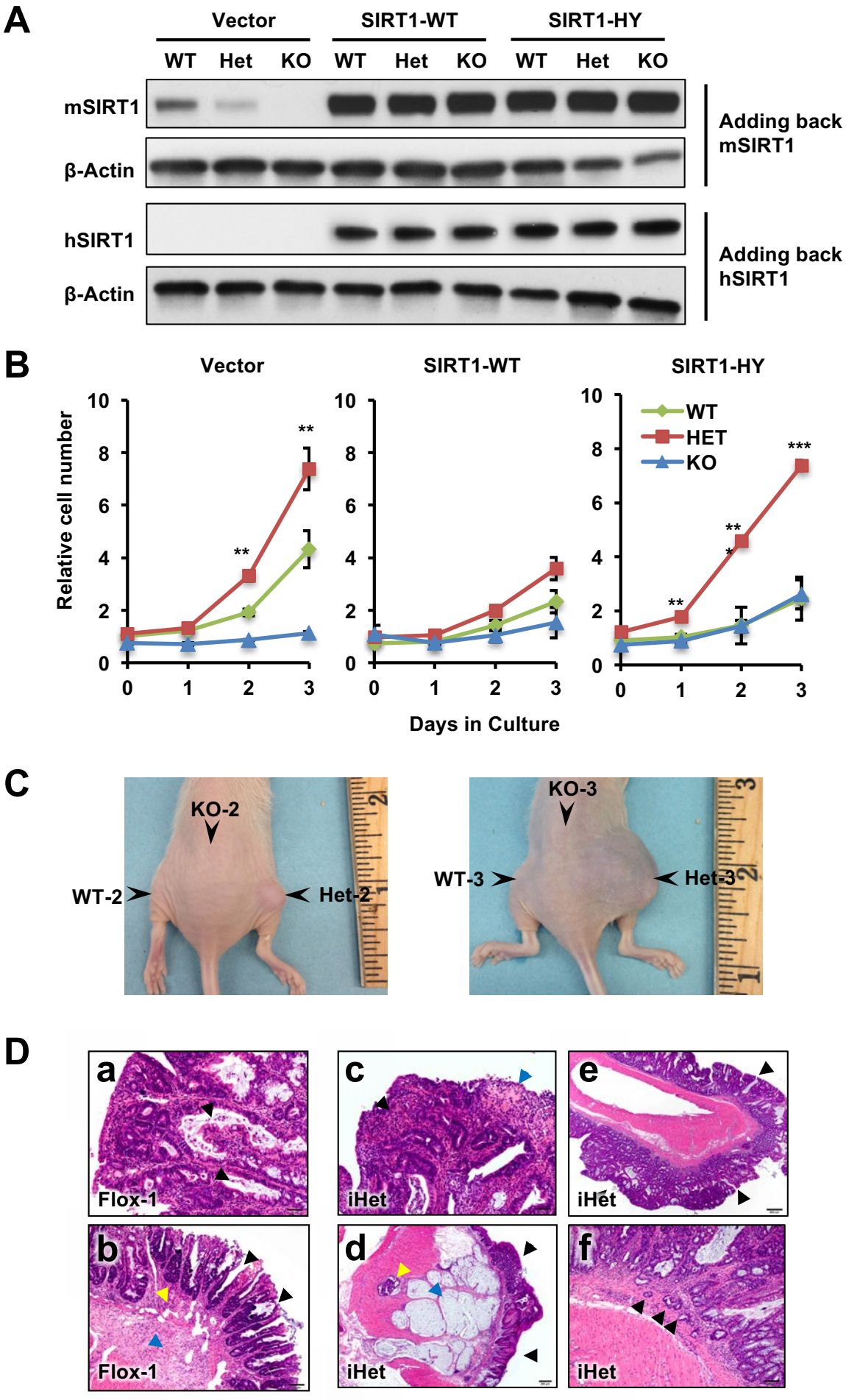
A
Vector
SIRT1-WT
SIRT1-HY
WT Het KO WT Het KO WT Het KO
mSIRT1
β-Actin
Adding back mSIRT1
hSIRT1
β-Actin
Adding back hSIRT1
B
Vector
SIRT1-WT
SIRT1-HY
Relative cell number
WT
HET
KO
Days in Culture
C
KO-2
WT-2
Het-2
KO-3
WT-3
Het-3
D
a
Flox-1
c
iHet
e
iHet
b
Flox-1
d
iHet
f
iHet

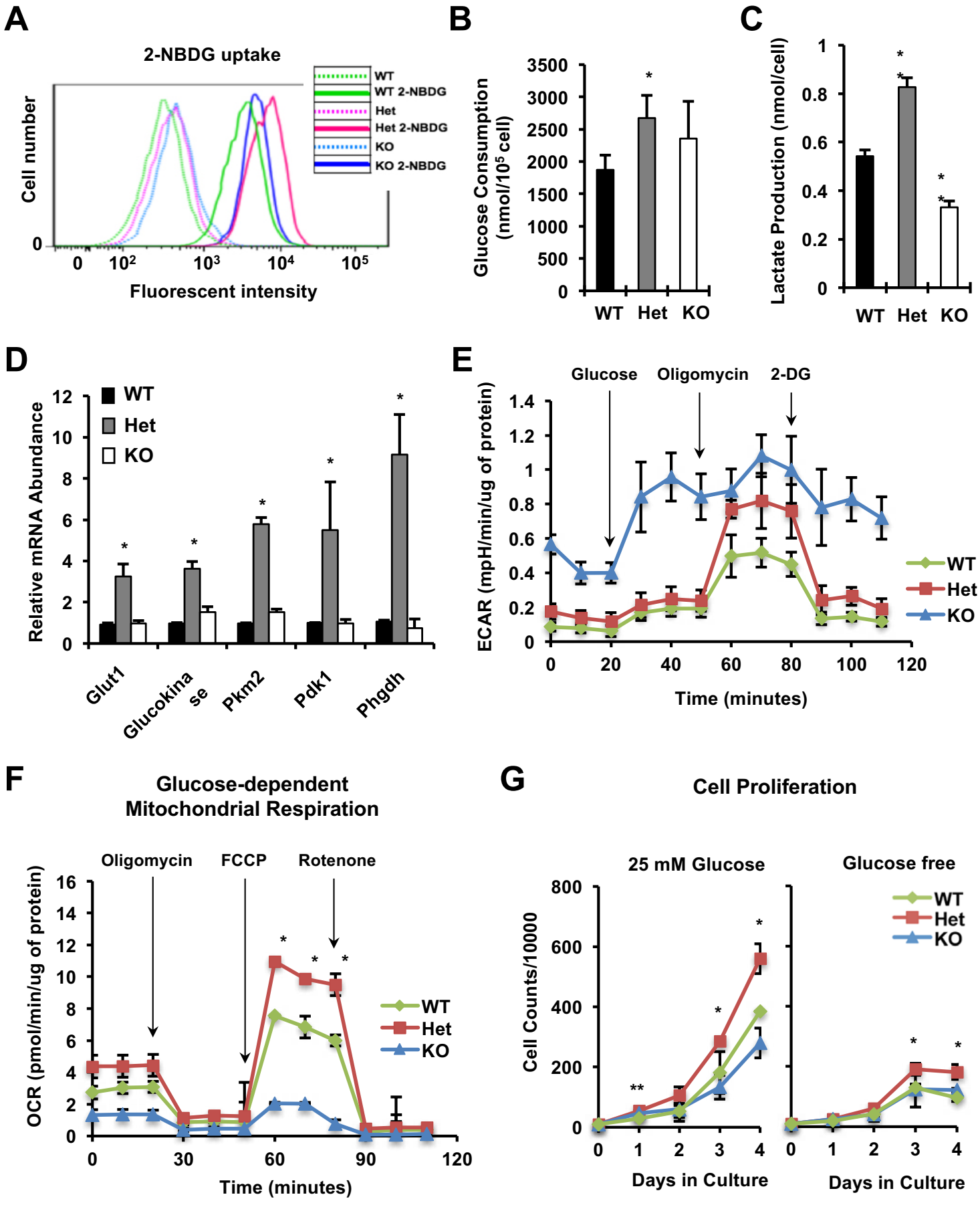
A
2-NBDG uptake
Cell number
Fluorescent intensity
WT
WT 2-NBDG
Het
Het 2-NBDG
KO
KO 2-NBDG
B
Glucose Consumption (nmol/10^5 cell)
WT
Het
KO
C
Lactate Production (nmol/cell)
WT
Het
KO
D
Relative mRNA Abundance
WT
Het
KO
Glut1
Glucokinase
Pkm2
Pdk1
Phgdh
E
Glucose
Oligomycin
2-DG
ECAR (mpH/min/ug of protein)
Time (minutes)
WT
Het
KO
F
Glucose-dependent Mitochondrial Respiration
Oligomycin
FCCP
Rotenone
OCR (pmol/min/ug of protein)
Time (minutes)
WT
Het
KO
G
Cell Proliferation
25 mM Glucose
Glucose free
Cell Counts/10000
Days in Culture
Days in Culture
WT
Het
KO

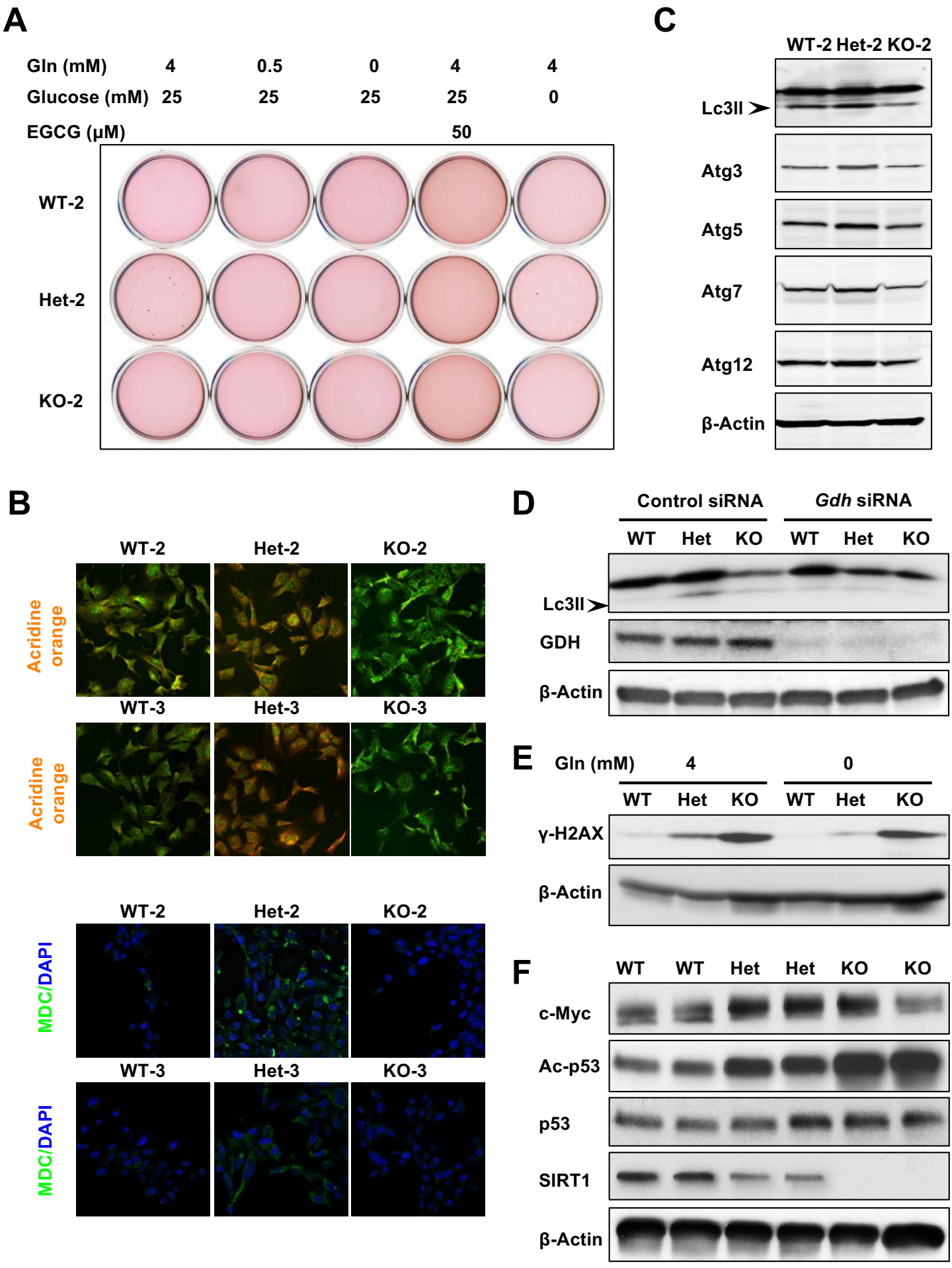
A
Gln (mM) 4 0.5 0 4 4
Glucose (mM) 25 25 25 25 0
EGCG (μM) 50
WT-2
Het-2
KO-2
C
WT-2 Het-2 KO-2
Lc3II
Atg3
Atg5
Atg7
Atg12
β-Actin
B
WT-2 Het-2 KO-2
Acridine orange
WT-3 Het-3 KO-3
Acridine orange
WT-2 Het-2 KO-2
MDC/DAPI
WT-3 Het-3 KO-3
MDC/DAPI
D
Control siRNA
Gdh siRNA
WT Het KO WT Het KO
Lc3II
GDH
β-Actin
E
Gln (mM) 4 0
WT Het KO WT Het KO
γ-H2AX
β-Actin
F
WT WT Het Het KO KO
c-Myc
Ac-p53
p53
SIRT1
β-Actin

A

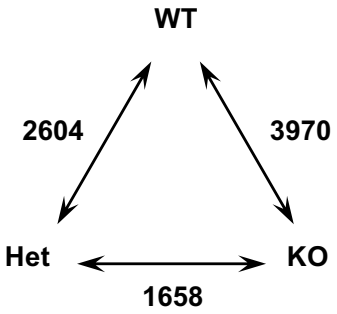

B

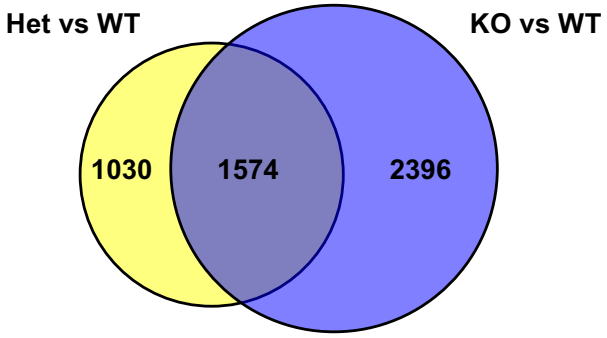

C

Unique for Het		Common		Unique for KO	
Regulator	**p-value**	**Regulator**	**p-value**	**Regulator**	**p-value**
Wnt3a	1.12E-07	Tp53	1.01E-16	Tretinoin (RA)	6.98E-07
Hdac	1.08E-06	Trim24	2.76E-13	F2	9.13E-06
Tnf	1.11E-06	Hras	1.06E-10	Tgfb1	2.87E-05
App	1.21E-06	Ifna2	1.49E-10	Ifnar	5.56E-05
Bmp7	1.23E-06	Ackr2	2.08E-10	Myc	6.52E-05

D

mTOR and MYC network

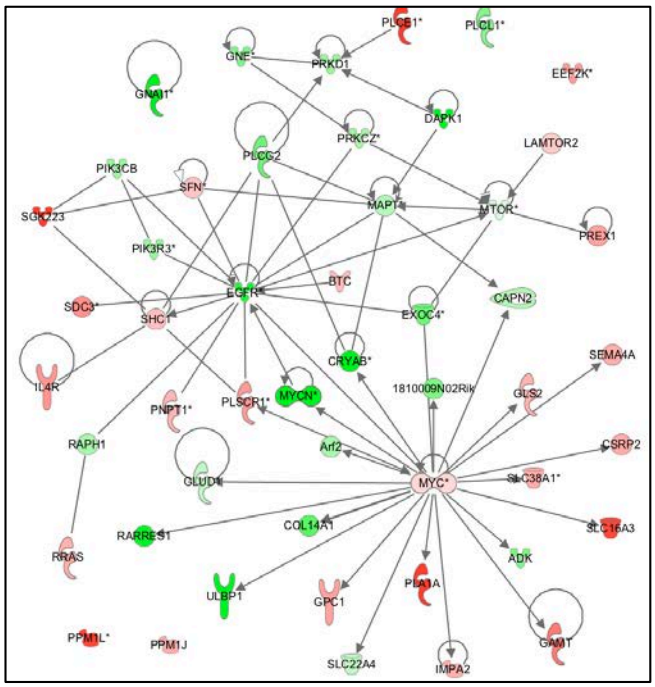

Het vs WT

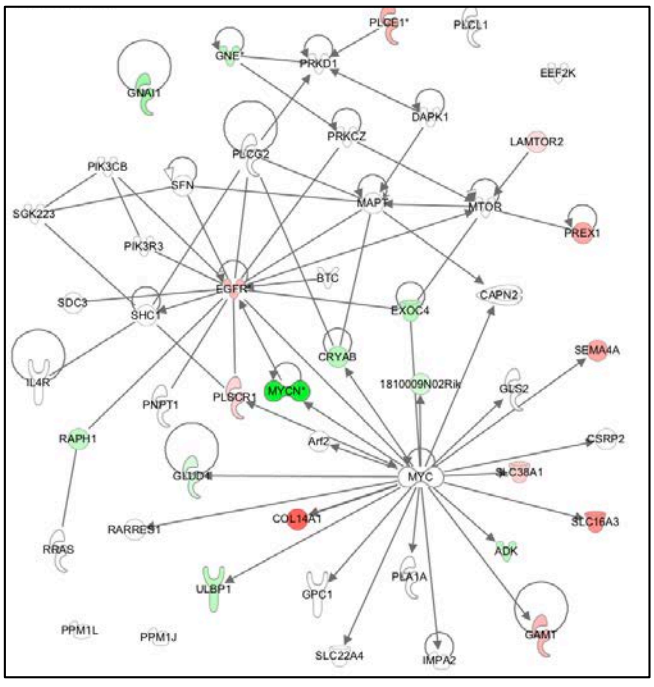

KO vs WT

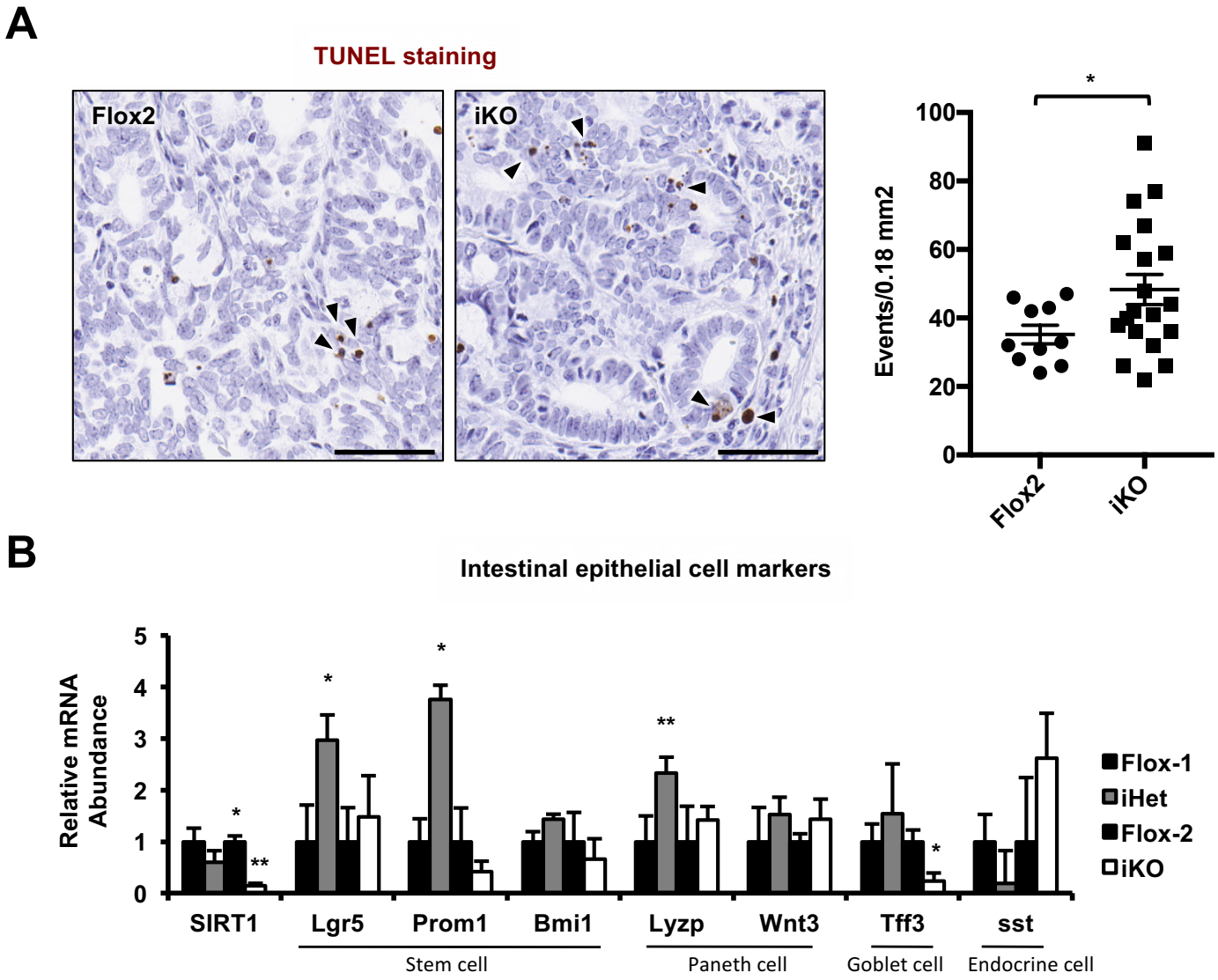
A
TUNEL staining
Flox2
iKO
Events/0.18 mm2
100
80
60
40
20
0
*
Flox2
iKO
B
Intestinal epithelial cell markers
Relative mRNA Abundance
5
4
3
2
1
0
*
**
*
*
**
*
SIRT1
Lgr5
Prom1
Bmi1
Lyzp
Wnt3
Tff3
sst
Stem cell
Paneth cell
Goblet cell
Endocrine cell
Flox-1
iHet
Flox-2
iKO

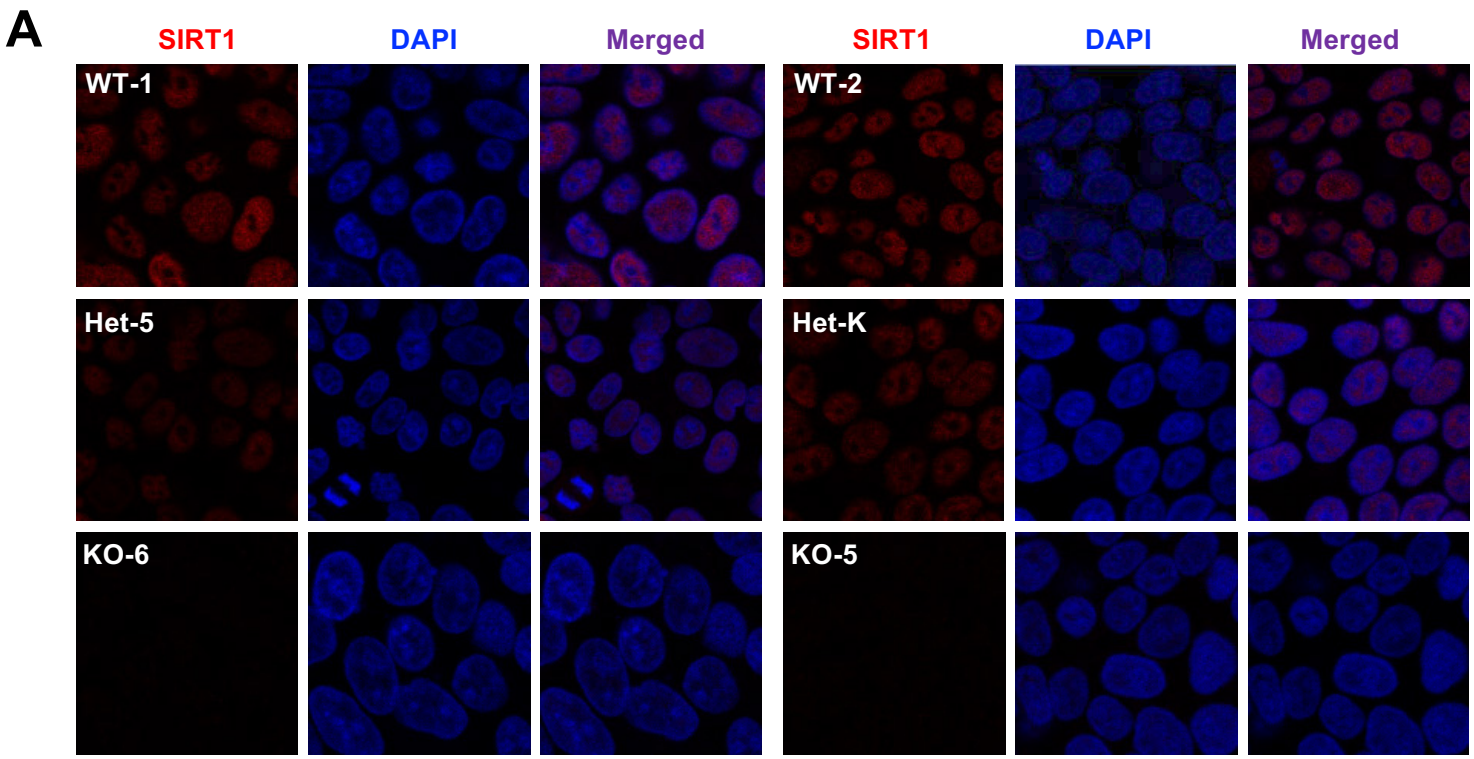
A
SIRT1
DAPI
Merged
SIRT1
DAPI
Merged
WT-1
WT-2
Het-5
Het-K
KO-6
KO-5

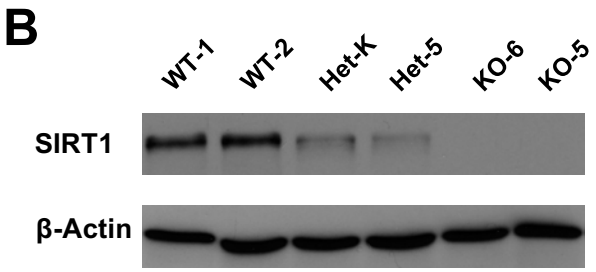
B
WT-1
WT-2
Het-K
Het-5
KO-6
KO-5
SIRT1
β-Actin

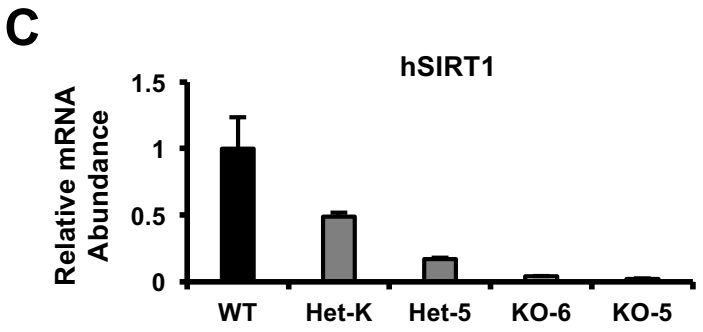
C
hSIRT1
Relative mRNA Abundance
1.5
1
0.5
0
WT
Het-K
Het-5
KO-6
KO-5

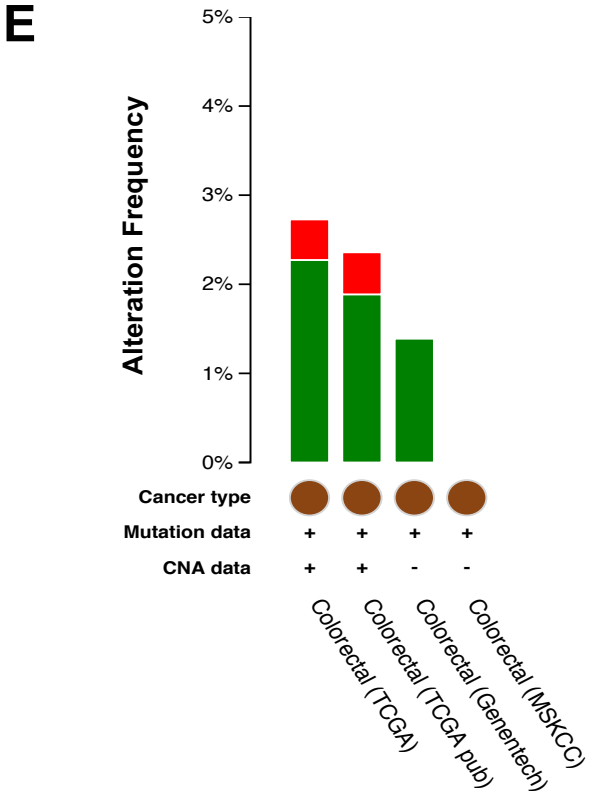
E
Alteration Frequency
5%
4%
3%
2%
1%
0%
Cancer type
Mutation data
CNA data
Colorectal (TCGA)
Colorectal (TCGA pub)
Colorectal (Genentech)
Colorectal (MSKCC)

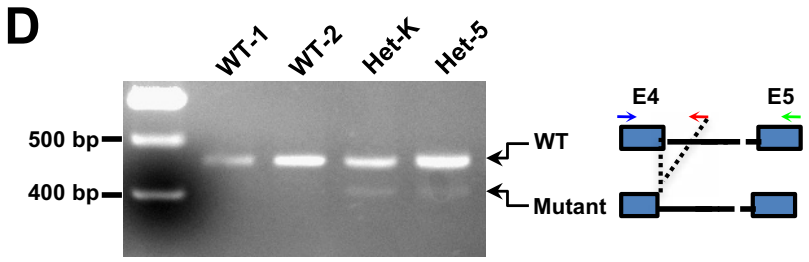
D
WT-1
WT-2
Het-K
Het-5
500 bp
400 bp
WT
Mutant
E4
E5

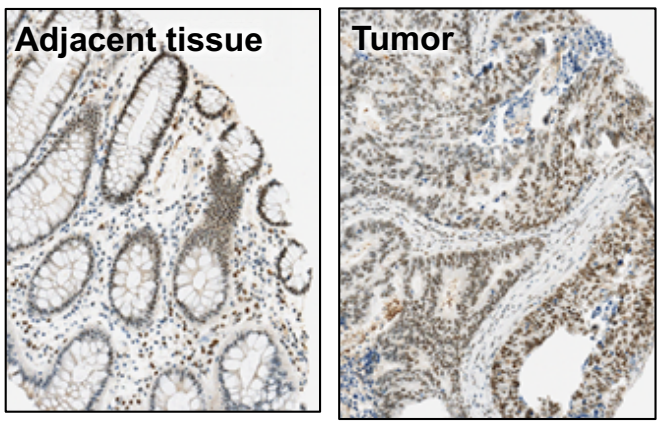
F
Adjacent tissue
Tumor

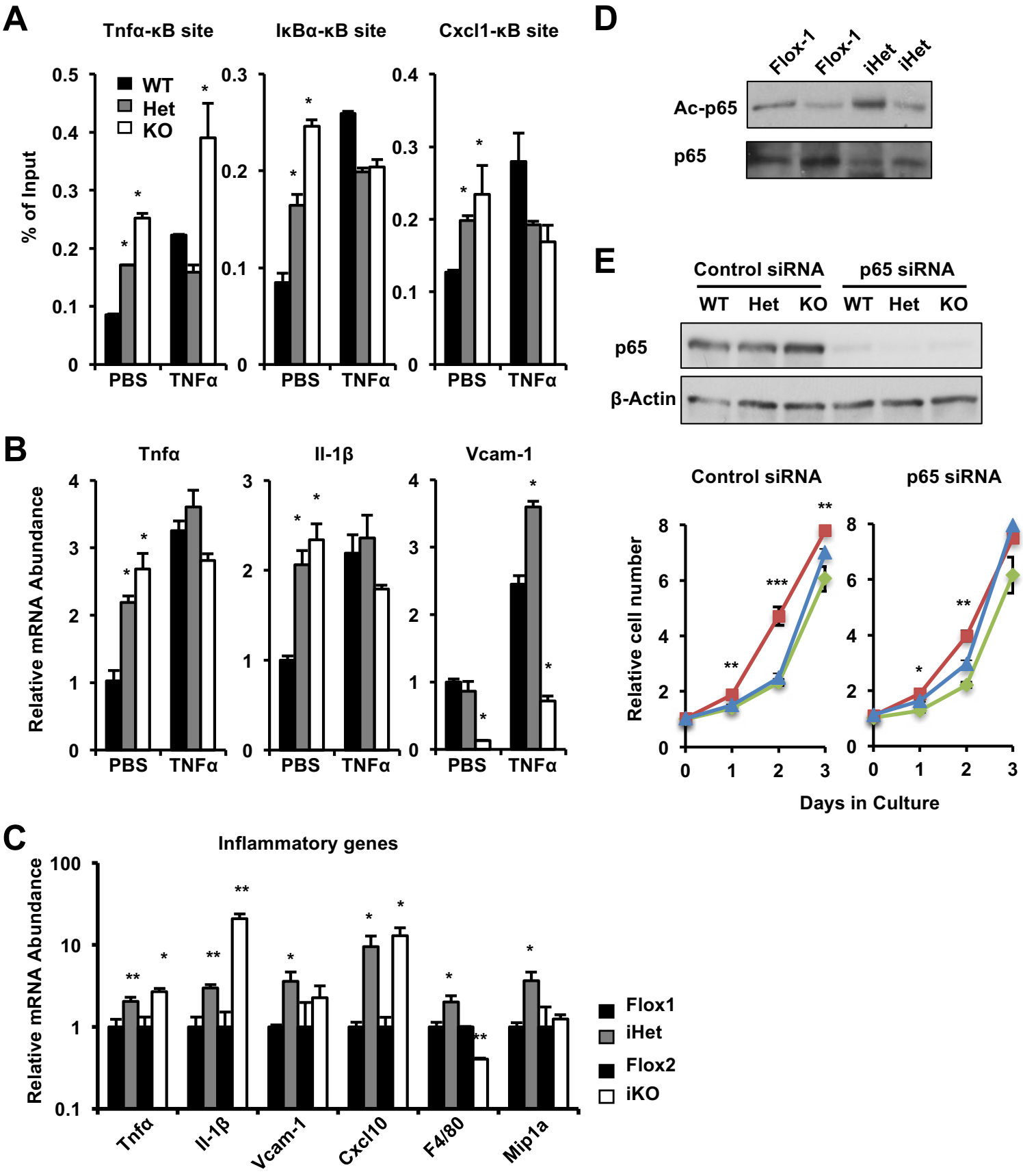
A
Tnfα-κB site
IκBα-κB site
Cxcl1-κB site
WT
Het
KO
% of Input
PBS
TNFα
B
Tnfα
Il-1β
Vcam-1
Relative mRNA Abundance
C
Inflammatory genes
Relative mRNA Abundance
Tnfα
Il-1β
Vcam-1
Cxcl10
F4/80
Mip1a
Flox1
iHet
Flox2
iKO
D
Flox-1
Flox-1
iHet
iHet
Ac-p65
p65
E
Control siRNA
p65 siRNA
WT
Het
KO
WT
Het
KO
p65
β-Actin
Control siRNA
p65 siRNA
Relative cell number
Days in Culture

Supplemental Figure Legends

Figure S1. Dosage-dependent effects of SIRT1 on cell proliferation and tumorigenesis. Related to Figure 1.

(A-B) Adding back WT SIRT1 but not SIRT1 HY mutant reduces the hyperproliferation of Het MEFs. WT, Het and KO MEFs were infected with lentiviruses expressing empty vector, WT, or HY mutant mouse or human SIRT1 proteins. The protein levels of SIRT1 in each line were analyzed by immunoblotting (A). n=4 (2 independent clones/each genotype, and 2 technical repeats), **p<0.01, ***p<0.001, values are represented as mean ± SEM.

(C) *Sirt1* Het MEFs readily form larger tumors in a xenograft model. Immortalized MEFs were injected subcutaneously into the flanks and back of host nude mice (Nu/J from Jax) and their tumorigenic potential was analyzed.

(D) Colon tumors from *Sirt1* iHet mice progressed into more advanced stages than those from control mice. Lesions from H&E staining of colon tumors from Flox-1 controls and *Sirt1* iHet mice were analyzed by a professional pathologist (E. Terence Adams). (a) Adenoma from a Flox-1 control mouse had irregular, dilated intestinal glands filled basophilic mucoid fibrillar material and degenerate cell debris (black arrows). Bar, 50 μm. (b) A Flox-1 control mouse had regenerative hyperplasia of intestinal glandular epithelium (black arrows) with fibrosis of the submucosa (blue arrows) and lamina propria (yellow arrows). Bar, 100 μm. (c) Mixed inflammatory infiltrate consisting of lymphocytes, neutrophils, and plasma cells in the lamina propria in tumors from a *Sirt1* iHet mouse. Bar, 50 μm. (d) Adenocarcinoma from a *Sirt1* iHet mouse with thick superficial squamous epithelium (black arrows), submucosal “mucinous lakes” (blue arrow), and invasive neoplastic glandular epithelium (yellow arrow). Bar, 200 μm. (e) Adenocarcinoma (black arrows) from a *Sirt1* iHet mouse. Bar, 500 μm. (f) Higher magnification of adenocarcinoma from e. Note aggregates of glandular epithelium invading the subjacent muscularis mucosa (black arrows). Bar, 100 μm.

Figure S2. Deletion of a single copy of *Sirt1* gene enhances aerobic glycolysis. Related to Figure 2 and 3.

((A) Het MEFs have increased glucose uptake. Immortalized MEFs were cultured in complete medium and uptake of 2-NBDG was analyzed as described in Experimental Procedures.

(B) Het MEFs have increased consumption of glucose from medium. Immortalized MEFs were cultured in complete medium and decrease of glucose from culture medium was analyzed as described in Experimental Procedures. n=3, *p<0.05, values are represented as mean ± SEM.

(C) Het MEFs have increased, whereas KO MEFs have reduced production of lactate. Immortalized MEFs were cultured in complete medium and release of lactate into culture medium was analyzed as described in Experimental Procedures. n=3, *p<0.05, values are represented as mean ± SEM.

(D) Het MEFs have increased expression levels of key genes involved in glucose and glycolysis when cultured in complete medium. mRNA abundance of indicated genes

were analyzed by quantitative real-time PCR (n=3, *p<0.05, values are represented as mean ± SEM).
(E) Het and KO MEFs have enhanced glycolysis. Glycolysis rates (ECAR) in WT, Het, and KO MEFs were analyzed as described in Experimental Procedures. n=5 technical repeats, values are represented as mean ± SEM. Please note that KO MEFs had an abnormally high basal glycolysis rate than WT and Het MEFs.
(F) Het MEFs have enhanced glucose-dependent mitochondrial respiration. Glucose-dependent OCR was determined as described in Experimental Procedures. n=5 technical repeats, *p<0.05, values are represented as mean ± SEM.
(G) Het MEFs display an enhanced proliferation rate in a glucose-free medium. Immortalized MEFs were cultured in normal DMEM medium with 25 mM glucose, 4 mM glutamine, and 10% FBS, or in a glucose-free DMEM. Cells were plated and counted at the indicated times. n=3, *p<0.05, **p<0.01, values are represented as mean ± SEM.

Figure S3. Haploinsufficiency of *Sirt1* promotes colony formation, autophagy, apoptosis resistance, and c-Myc overexpression. Related to Figure 3, 4, and 5.
(A) The distinct colony formation abilities of WT, Het, and KO MEFs on soft agar are dependent on the cellular glutaminolysis activity. Data were from the second set of WT, Het, and KO MEFs.
(B) Het MEFs enhances yet KO MEFs reduces formation of acidic autophagolysosomes (acridine orange staining, top six panels) and autolysosomes (Monodansylcadaverine staining, MDC, bottom six panels) in complete glutamine-containing medium. Representative images from the other two sets of MEFs were shown.
(C) Het MEFs have increased levels of protein factors involved in augophagy. Protein levels of indicated factors were analyzed by immuno-blotting. Data were from the second set of WT, Het, and KO MEFs.
(D) The enhanced autophagic events in Het MEFs are dependent on glutaminolysis. GDH was knocked down by siRNAs in WT, Het, or KO MEFs and cultured in the complete medium. The expression of Lc3II was analyzed by immuno-blotting.
(E) KO MEFs have increased DNA damage after etoposide treatment in both complete and glutamin free media. Immortalized MEFs were treated with 10 μM etiposide for 48 hours in DMEM medium containing 4 mM or 0 mM of glutamine. The degree of DNA damage was monitored by the levels of a double strand break marker, γ-H2AX.
(F) Acetylation of p53 and expression of c-Myc in the other two sets of WT, Het, and KO MEFs. Immortalized MEFs cultured in complete glutamine-containing medium were treated with 5 μM TSA for 30 minutes, and the total levels and acetylation levels of indicated proteins were analyzed by immuno-blotting.

Figure S4. WT, Het, and KO MEFs have distinct gene expression profiles. Related to Figure 5.
(A) The numbers of differentially expressed gene probes between WT, Het, and KO MEFs in normal culture medium. The mRNAs were analyzed by the mouse whole

genome microarrays as described in Experimental Procedures (n=4 independent cell lines/genotype, adjusted $p<0.05$).
(B) Venn-diagram representation of significantly altered gene probes between Het vs WT and KO vs WT.
(C) Het and KO MEFs have distinct activities of indicated upstream regulators. Common gene list form Het and KO MEFs as well as unique gene lists from Het and KO MEFs were analyzed by the IPA software, and the predicted top 5 altered upstream regulators in each gene list were listed (n=4 independent cell lines/genotype). Green, repressed regulators; red, activated regulators.
(D) Het but not KO MEFs have significant alteration in the mTOR/MYC networks. The significantly altered gene probes in SIRT1 Het vs WT (left) or in SIRT1 KO vs WT (right) were analyzed by the IPA software. Green, decreased in HET (left) or KO (right); red, increased in HET (left) or KO (right).

Figure S5. *Sirt1* iHet colon tumors have increased apoptosis and mRNA levels of markers for intestinal stem cells. Related to Figure 6.
(A) Colon tumors from *Sirt1* iKO mice have increased apoptosis. Apoptosis events were detected by TUNEL staining (Bars, 50 μm). n=4 mice/genotype, and apoptotic events were quantified in random selected fields. *$p<0.05$, values are represented as mean ± SEM.
(B) *Sirt1* iHet colon tumors have mRNA levels of markers for intestinal stem cells. n=6 mice/genotype, *$p<0.05$, **$p<0.01$, values are represented as mean ± SEM.

Figure S6. Dose-dependent effect of SIRT1 on colon cancer development in humans. Related to Figure 7.
(A-B) Generation of DLD1 *SIRT1* WT, Het, and KO cells. DLD1 cells were transiently transfected with Cas9WT mammalian expression vectors expressing gRNAs targeting exon 4-intron 4 (AAAGgtactatgaactcttc, for generation of Het cells) or exon 5 (GGACAATTCCAGCCATCTCTCT, for generation of KO cells) of human *SIRT1* gene. Cell clones with deletion of one copy (*SIRT1*$^{+/-}$, Het) or both copies (*SIRT1*$^{-/-}$, KO) of human *SIRT1* gene were identified by immunofluorescent staining (A), and immuno-blotting analysis (B).
(C-D) The genotypes of DLD1 *SIRT1* WT, Het, and KO cells were confirmed by real-time PCR analysis of mRNA (C) and genomic DNA PCR analysis of gene loci alteration (D). In (C), real-time PCR analyses were performed using primers flanking exon4 (blue) and exon 5 (green) against cDNA. In (D), PCR reactions were performed using primers flanking the exon 4 (blue) and the first 299 nt of the intron 4 (red) against genomic DNA. Subsequent sequencing analyses of the resulting PCR fragments revealed that Het-K cells have a WT allele and a mutant allele with deletion of 45 nt at the junction of exon 4 and intron 4 (including the last 5 nt of exon 4 and the first 40 nt of intron 4), while Het-5 cells have a WT allele and a mutant allele with deletion of 49 nt at the junction of exon 4 and intron 4 (including the last 4 nt of exon 4 and the first 45 nt of intron 4).
(E) Alteration Frequency of human *SIRT1* gene in colorectal cancer patients. Analysis was performed via http://www.cbioportal.org/index.do, from four

independent studies with total of 1117 colorectal adenocarcinoma samples. Red, gene amplification; Green, gene mutation. Please also see Table S2.
(F) Representative examples of SIRT1 protein IHC staining in paired adjacent tissue and tumor tissue. Immunohistochemistry was performed at Translational Pathology Laboratory at the University of North Carolina at Chapel Hill using a human SIRT1 specific rabbit polyclonal antibody.

Figure S7. SIRT1 haploinsufficiency activates the NF-κB pathway and inflammation *in vitro* and *in vivo*. Related to Figure 5.
(A) Single-copy deletion of *Sirt1* enhances recruitment of p65 subunit of NF-κB to its target promoters. Immortalized MEFs cultured in complete glutamine-containing medium were treated with 10 ng/ml of TNFα for 30 min in PBS (as control). The promoter associated p65 levels were analyzed by Chromatin immunoprecipitation as described in Experimental Procedures (n=3 technical repeats, *p<0.05, values are represented as mean ± SEM).
(B) Single-copy deletion of *Sirt1* is sufficient to activate the cellular NF-κB pathway. Immortalized MEFs were cultured and treated as in (B), and the mRNA levels of indicated NF-κB target genes were analyzed by q-PCR (n=3 technical repeats, *p<0.05, values are represented as mean ± SEM).
(C) Both *Sirt1* iHet and iKO colon tumors have increased expression of inflammatory genes. n=6 mice/group, *p<0.05, **p<0.01, values are represented as mean ± SEM.
(D) *Sirt1* iHet colon tumors have enhanced acetylation of p65.
(E) Knocking down of p65 does not significantly eliminate hyper-proliferation of Het MEFs. p65 was knocked down by siRNAs in WT, Het, or KO MEFs (n=5 technical repeats, **p<0.01, *p<0.05, values are represented as mean ± SEM).

Table S1. Alterations of human SIRT1 gene in colorectal adenocarcinoma. Related to Figure 7

STUDY_ABBREVIATION	STUDY_NAME	NUM_OF_CASES_ALTERED	PERCENT_CASES_ALTERED	TOTAL_CASES
Colorectal (TCGA)	Colorectal Adenocarcinoma (TCGA, Provisional)	6	2.70%	631
Colorectal (TCGA pub)	Colorectal Adenocarcinoma (TCGA, Nature 2012)	5	2.40%	276
Colorectal (Genentech)	Colorectal Adenocarcinoma (Genentech, Nature 2012)	1	1.40%	72
Colorectal (MSKCC)	Colorectal Adenocarcinoma Triplets (MSKCC, Genome Biology 2014)	0	0%	138

Note: Analysis is performed via http://www.cbioportal.org/index.do on 5/4/2016

Table S2. Subject Characteristics (n=348). Related to Figure 7.

Characteristic	Mean	SD
Age at Diagnosis (years)	66.8	13.1
	N	**%[a]**
Sex		
Male	170	49%
Female	178	51%
Race		
Non-Hispanic White	277	80%
Black	60	17%
Native American	4	1%
Asian	2	1%
Hispanic or Latino	2	1%
More than one race	3	1%
Tumor Stage		
Local	163	49%
Regional	125	37%
Distant	47	14%
Missing	13	
Histologic Grade		
Well/Moderately Differentiated	243	83%
Poorly/Not Differentiated	50	17%
Missing	55	
Died Within 5 Years of Surgery	123	35%

[a]Percentages are for non-missing data.

Table S3. Average continuous SIRT1 expression in subjects overall and in various subsets (scale: H scores, 0-300). Related to Figure 7.

Subjects	Tissue Type	N	25th Percentile	Median	75th Percentile	Mean	SD	P-value[a]
Overall	Tumor	348	141	187	236	181	69	0.5
	Adjacent	290	135	191	230	178	65	
Male	Tumor	170	135	180	232	175	68	0.8
	Adjacent	148	132	190	227	177	62	
Female	Tumor	178	146	199	243	187	70	0.3
	Adjacent	142	140	192	238	178	68	
White	Tumor	277	141	190	236	181	69	0.6
	Adjacent	232	135	190	231	178	66	
Non-White	Tumor	71	142	184	239	181	69	0.7
	Adjacent	58	135	192	228	176	61	
Under 68	Tumor	175	139	187	236	181	67	0.4
	Adjacent	147	133	188	226	176	63	
At Least 68	Tumor	173	145	188	237	181	71	0.9
	Adjacent	143	135	192	236	180	67	
Stage I/II	Tumor	163	143	187	239	181	71	0.1
	Adjacent	129	116	185	226	169	69	
Stage III/IV	Tumor	172	141	189	236	183	67	0.6
	Adjacent	149	152	194	238	186	60	

[a]Comparisons of means using unpaired two-sample t-tests.

Supplemental Experimental Procedures

Cell culture

Primary mouse embryonic fibroblasts (MEFs) were generated from E14.5 day old embryos from the whole body *Sirt1* heterozygous knockout mice breeding (on a C57BL/6 background) [S1]. Three independent groups of littermate *Sirt1* wild type (*Sirt1*$^{+/+}$, WT), heterozygous (*Sirt1*$^{+/-}$, Het), and knockout (*Sirt1*$^{-/-}$, KO) MEFs were immortalized by overexpressing SV40T. Immortalized MEFs were then cultured in DMEM medium with 10% FBS together with indicated amounts of glucose and glutamine.

Human Dukes' type C colorectal adenocarcinoma cell line, DLD1, was transiently transfected with Cas9WT mammalian expression vectors expressing gRNAs targeting exon 4-intron 4 (AAAGgtactatgaactcttc, the deletion efficiency is around 30%, used for generation of Het cells) or exon 5 (GGACAATTCCAGCCATCTCTCT, the deletion efficiency is about 90%, used for generation of KO cells) of human *SIRT1* gene (Horizon Discovery, Cambridge, UK). Cell clones with deletion of one copy (*SIRT1*$^{+/-}$, Het) or both copies (*SIRT1*$^{-/-}$, KO) of human *SIRT1* gene were identified by immunofluorescent staining and immuno-blotting analysis, and confirmed by genomic DNA PCR and sequencing. Cells were then cultured in RPMI1640 medium with 10% FBS together with indicated amounts of glucose and glutamine.

Cell proliferation assay

Five thousand cells were plated in 96-well plates per well at 50% confluence overnight. Cell viability was determined with the CellTiter 96® AQueous Non-Radioactive Cell Proliferation Assay Kit from Promega according to the manufacturer's protocol. To deprive glucose or glutamine, cells were plated in complete culture media, which was exchanged with glucose-free or glutamine-free medium supplemented with 10% FBS the following day. Media were not changed throughout the course of the experiment.

Clonogenic assay

Soft agar was conducted as previously described [S2]. It was used to measure the ability of cells to grow in an anchorage-independent manner, a common characteristic of cancer cells. Briefly, 2 ml of 0.5% agar medium were plated in 35 mm dishes and allowed to harden at room temperature under sterile conditions for 20 min. Cells were subcultured and filtered through a 40-μm pore size cell strainer to obtain a single-cell suspension. A cell suspension of 37,500 cells/ml of 10% FBS in growth medium was gently mixed with 2 ml of 0.5% agar medium, giving 0.33% agar in the medium. This suspension was layered on top of the hardened agar in 35 mm plates, giving 12,500 cells/plate. Plates were incubated at 37°C in humidified atmosphere and not fed during the 21 day incubation period. Colonies were then stained with p-iodonitro-tetrazolium overnight at 37°C, fixed with 0.5 ml 10% buffered formalin and immediately counted. Four dishes were plated for each cell line/condition.

Xenograft studies

Half million *Sirt1* WT, Het, or KO MEFs in 0.1 ml of sterile PBS were subcutaneously injected in the flanks (both sides) and back of host nude mice (Nu/J from Jackson Laboratories). Each of three sites in one mouse was injected with one genotype respectively so that tumors from MEFs with three Sirt1 genotypes were compared from the same mouse. Mice were checked for the appearance of tumors weekly and the tumors were harvested when the biggest one reached 10 mm in size.

Glutamine and Glucose Measurements

Glucose, lactate and ammonia levels in culture media were measured using the Glucose (GO) Assay Kit (GAGO20, Sigma, St. Louis. MO), the Lactate Assay Kit (MAK064, Sigma, St. Louis. MO) and the Ammonia Assay Kit (AA0100, Sigma, St. Louis. MO), respectively. The cellular glutamine level was detected by the Glutamine and Glutamate Determination Kit (GLN1, Sigma, St. Louis. MO). The cellular α-Ketoglutarate and glutamate were detected by α-Ketoglutarate Assay Kit (MAK054, Sigma, St. Louis. MO) and Glutamate Assay Kit (ab83389, Abcam, Cambridge, MA), separately. The glutamate dehydrogenase (GDH) was measured by GDH Activity Assay Kit (MAK099, Sigma, St. Louis. MO).

Detection of Acidic Vesicular Organelles (AVOs) by Acridine Orange Staining

Acridine orange (Sigma) was added at a final concentration of 1 μg/ml for a period of 15 min at 37°C on eight-well microscopy slides. The stained cells were then washed twice with phosphate-buffered saline (PBS). Detection of fluorescence signal was performed with a confocal fluorescence microscope (Nikon EZ-C1, Nikon).

Visualization of MDC-labeled vacuoles

Autophagic vacuoles were labeled with monodansylcadaverine (MDC, 30432 Sigma) by incubating cells grown on eight-well microscopy slides with 0.05 mM MDC in PBS at 37°C for 10 minutes. After incubation, cells were washed four times with PBS and immediately analyzed by fluorescence microscopy using a confocal fluorescence microscope (Nikon EZ-C1, Nikon).

Protein acetylation analysis

To analyze the acetylation levels of p65, c-Myc, β-catenin in cells, WT, Het, and KO MEFs were cultured in complete medium. The total cell extracts were immunopurified with antibodies against p65 (Santa Cruz Technology, Santa Cruz, CA), c-Myc (Cell Signaling Technology, Danvers, MA), or β-catenin (GeneTex, Irvine, CA). The acetylation levels of purified proteins were analyzed with anti-acetyl-lysine polyclonal antibodies (Cell Signaling Technology, Danvers, MA).

Microarray study and data analysis

To analyze the transcriptomes of immortalized mouse embryonic fibroblasts (MEFs), total RNA was isolated using the Qiagen RNeasy mini-kit, and gene expression profiles were analyzed using Agilent Whole Mouse Genome 4x44 multiplex format oligo arrays (014868) (Agilent Technologies, Santa Clara, CA), following the Agilent 1-color microarray-based gene expression analysis protocol.

Data were obtained using Agilent Feature Extraction software (v9.5), using the 1-color defaults for all parameters. The Agilent Feature Extraction Software performed error modeling, adjusting for additive and multiplicative noise. The microarray data are available in the Gene Expression Omnibus repository at the National Center for Biotechnology Information and the GEO accession is GSE76088: (http://www.ncbi.nlm.nih.gov/geo/query/acc.cgi?token=ifwzqeuybfilxuz&acc=GSE76088).

To further analyze the microarray datasets, data were processed using Agi4x44PreProcess, limma in Bioconductor for the R software environment (www.rproject. org). A single log scale normalized expression measure for each probes set was obtained after background correction and normalization between samples. Box plots, density plots, MA plot and spatial images of the raw and normalized data were examined in order to check the quality of the microarray data, and that no unusual results for any slide were observed. Principal Component analysis (PCA) was performed on all samples and all probes sets to reduce the dimensionality of the data while preserving variation. This allowed assessment of the similarities and differences of samples within and between treatment groups. The significance of the log ratio for each probe was determined by calculating a modified t statistic per probe using an empirical Bayesian approach. Probes that had a Benjamini-Hochberg multiple test corrected p value ($p<0.05$) were considered to be differentially expressed. The lists of probe sets were further analyzed in the Ingenuity Pathway Analysis tool (version 21901358) (Ingenuity Systems, Redwood City, CA).

SIRT1 expression in clinical tissue specimens

To assess the clinical value of SIRT1, we measured protein expression using immunohistochemistry (IHC) (rabbit polyclonal antibody [cat #2493] from Cell Signaling Technology [Danvers, MA]) in tissue microarrays constructed for the North Carolina site of the Cancer Care Outcomes Research and Surveillance Consortium (CanCORS).

IHC was performed at the Translational Pathology Laboratory at the University of North Carolina at Chapel Hill using the Bond fully-automated slide staining system (Leica Microsystems Inc., Norwell, MA). Slides were deparaffinized in Bond Dewax solution (AR9222) and hydrated in Bond Wash solution (AR9590). Antigen retrieval was performed at 100°C for 20 minutes at 100°C in solution 2 at pH 9.0 (AR9640). After pretreatment, anti-SIRT1 was applied for 4 hours at room temperature.

Detection of SIRT1 was performed using the Bond Polymer Refine Detection System (DS9800). Stained slides were dehydrated and cover-slipped. Positive and negative controls (no primary antibody) were included for each antibody. Stained slides were digitally imaged at 20x magnification using the Aperio ScanScope XT (Aperio Technologies, Vista, CA). Images were stored in the Aperio Spectrum Database.

Digital image analysis yielded continuous marker expression data on several scales: average intensities (0-3), percent positive nuclei (0-100), and H scores (0-300). Most subjects had multiple tissue microarray cores for each tissue type (tumor or normal) per subject. To account for replicate cores, a single marker expression value was derived for each subject by tissue type by taking a weighted average of

cores, with the number of nuclei in each core serving as the weights. Using unpaired two-sample t-tests, SIRT1 expression in tumor tissue was compared to expression in normal tissue for overall subjects as well as by sex, race, age (dichotomizing at the median age of 68), and by tumor stage (I/II or III/IV).

Supplemental References

S1. McBurney, M.W., Yang, X., Jardine, K., Hixon, M., Boekelheide, K., Webb, J.R., Lansdorp, P.M., and Lemieux, M. (2003). The mammalian SIR2alpha protein has a role in embryogenesis and gametogenesis. Mol Cell Biol *23*, 38-54.

S2. Tokar, E.J., and Webber, M.M. (2005). Cholecalciferol (vitamin D3) inhibits growth and invasion by up-regulating nuclear receptors and 25-hydroxylase (CYP27A1) in human prostate cancer cells. Clin Exp Metastasis *22*, 275-284.